atmosphere

MDPI

Article

Geothermal Energy Potential for Cooling/Heating Greenhouses in Hot Arid Regions

Ibrahim Al-Helal [1], Abdullah Alsadon [2], Samy Marey [3], Abdullah Ibrahim [2], Mohamed Shady [1] and Ahmed Abdel-Ghany [1,4,*]

1 Department of Agricultural Engineering, College of Food and Agriculture Sciences, King Saud University, P.O. Box 2460, Riyadh 11451, Saudi Arabia; imhelal@ksu.edu.sa (I.A.-H.); mshady@ksu.edu.sa (M.S.)
2 Department of Plant Production, College of Food and Agriculture Sciences, King Saud University, P.O. Box 2460, Riyadh 11451, Saudi Arabia; alsadon@ksu.edu.sa (A.A.); adrahim@ksu.edu.sa (A.I.)
3 Sciences, Technology and Innovation Unit, King Saud University, P.O. Box 2454, Riyadh 11451, Saudi Arabia; samarey@ksu.edu.sa
4 Mechanical Power Engineering Department, Faculty of Energy Engineering, Aswan University, Aswan 8510, Egypt
* Correspondence: aghany@ksu.edu.sa or aghany@energy.aswu.edu.eg

Abstract: In arid regions, drastic seasonal variations in the climatic parameters are common; thus, a high potential of geothermal effects for heating/cooling applications is expected. However, such applications are very limited in these regions due to the lack of information about underground temperature profiles of the surface and shallow zones. Therefore, this study aims to (i) measure the underground temperature profile for one year to determine the optimum depth for burying EAHE pipes; (ii) examine the possibility of water vapour condensation occurring in the buried EAHE pipes, if the air let into the pipes was humid; and (iii) quantify the maximum cooling/heating capacity, if an EAHE was implemented. The results show that a 3-m depth is optimal to bury EAHE pipes, where the ground temperature is 32 °C in the summer and 29 °C in the winter. These temperatures would provide a maximum cooling/heating capacity of 1000/890 MJ day^{-1} for each 1 m^3 of humid air exhausted from a greenhouse. If the EAHE were to operate in a closed loop with a greenhouse, the condensation of water vapour in the EAHE pipes would be impossible during the cooling process. The results of this study are useful for designers using geothermal effects for indoor space cooling and heating in arid regions.

Keywords: arid climate; geothermal energy; underground temperature; greenhouse; heat exchanger

check for updates

Citation: Al-Helal, I.; Alsadon, A.; Marey, S.; Ibrahim, A.; Shady, M.; Abdel-Ghany, A. Geothermal Energy Potential for Cooling/Heating Greenhouses in Hot Arid Regions. *Atmosphere* **2022**, *13*, 105. https://doi.org/10.3390/atmos13010105

Academic Editors: Zengyun Hu, Xuguang Tang and Qinchuan Xin

Received: 10 December 2021
Accepted: 5 January 2022
Published: 10 January 2022

1. Introduction

The use of greenhouses in arid areas, such as in the Arabian Peninsula, faces serious obstacles due to the extremely harsh environment; daytime overheating caused by intensive solar irradiance and night-time unfavourable undercooling are common weather conditions in desert areas [1]. By solving greenhouse operational problems (cooling in summer days and heating in winter nights), farmers can grow protected crops throughout the year.

Evaporative cooling (wet pad–fan systems) and fuel burners are commonly used for cooling and heating greenhouse air, whereby cold humid air (in summer) and warm air (in winter) are exhausted from the greenhouse and lost to the surrounding (useless air) during ventilation processes. Moreover, heating and evaporative cooling systems are an additional burden of energy and water consumption in greenhouses [2]. To overcome these difficulties, a semi-closed greenhouse has been suggested, where the inside greenhouse air is circulated in a closed loop and its cooling or heating are obtained by using sustainable energy resources. Looking for low-cost, energy- and water-saving techniques for heating/cooling inside greenhouse air is an essential priority for sustainable agriculture and the development of the rural areas in arid regions [3]. Therefore, a semi-closed greenhouse coupled with an earth–air heat exchanger (EAHE) was suggested in the Kingdom of Saudi Arabia (KSA). The EAHE is expected to be an effective way for heating/cooling greenhouses in the deserts characterised by hot arid climates. This is because the extracted low-grade geothermal energy (fluid temperature < 100 °C) as a sustainable energy resource is applicable for different purposes, such as desalination; drying technology; heating and cooling load production, using single-effect lithium bromide absorption chillers; agriculture greenhouses; and domestic use [4]. On the other hand, high-grade geothermal energy is applicable for power generation based on the Rankin cycle concept [5,6].

Even though the KSA is considered one of the most geothermally active countries in the Middle East [7], there is a lack of studies that address the issues of geothermal energy potential and its applications in the KSA [8]. Very few studies can be found that discuss the geothermal activity in the KSA from a geological science point of view [7,8]. Moreover, the geothermal energy potential, as well as the underground temperature profile in the shallow zone (0~8 m), has never been measured or evaluated in the KSA desert. Specifically, accurate information about the vertical distribution of soil temperature and geothermal energy potential in the shallow zone are still missing relatively to the KSA desert.

It is well known that the earth strongly absorbs solar energy during the daytime and stores a considerable amount of thermal energy at a particular depth. This is mainly attributable to the high solar irradiance intensity and large heat capacity of the soil. According to the diurnal variation in solar irradiance and ambient air temperature, the maximum temperature oscillation occurs at the Earth's surface, and it varies with the depth inside the Earth. Many researchers have measured the temperature distribution with depth and found that the oscillation of temperature below the ground attenuated with depth and became constant at a particular depth. For example, at a 0.18-m depth, the daily average soil temperature was 17.84 °C in the winter and 32.87 °C in the summer in New Delhi, India [9]. Moreover, the annual average temperatures of soil were measured at a 4-m depth and under different conditions of the ground surface in New Delhi, India. It was 29 °C when the ground surface was exposed to solar radiation, 19 °C when the ground surface was wetted, and 17 °C when the ground surface was wetted and shaded [9]. Different values of the annual average temperature of different soils in different places worldwide have been measured at different depths and reported in the literature, e.g., 23.45 °C at a 4-m depth in Las Vegas, USA [10]; 27–28 °C at a 2.5-m depth under warm humid weather conditions in Mexico City [11]; 18.7 °C at a 2-m depth and 20 °C at a 4-m depth in Brazil [12]; 25 °C at a 2-m depth in Bhopal, India [13]; 11.5 °C in winter and 17.5 °C in summer at a 2-m depth in Tianjin, China [14]; and 17.6 °C at a 3.6-m depth in Shouguang City, China [15]. In a typical arid climate (the desert in the south part of Algeria), the underground temperature was measured, in the hottest month in summer, to be 30 °C at a 2-m depth and 27 °C at a 5-m depth [16]. These temperatures are usually defined as ground undisturbed temperatures (GUTs). The GUT at a certain depth in the ground is nearly constant during the day and night and throughout the year. This depends on the groundwater level, the physical/chemical properties of soil and the ground surface conditions (mainly solar radiation flux and ambient air temperature). For greenhouse applications, the GUTs reported in the literature are reasonable for heating and cooling greenhouses; further, they can be used for indoor space heating and cooling (e.g., residential buildings, poultry houses, livestock houses, etc.) [17]. However, the cost of digging to the optimum depth for availing free geothermal energy should be considered; this depends on the type and nature of the soil. Besides the sustainability and low-cost and/or free geothermal energy for heating/cooling greenhouses, it can also be recognized that the thermal load levelling of the underground temperature at a depth from 2.5 m to 4 m is very low and is required for plants' healthy growth, irrespective of any climatic condition [17,18]. To use the geothermal energy potential for cooling/heating greenhouses in a closed loop, Polyvinyl Chloride (PVC) or High-density Polyethylene (HDPE) pipes are an optimum choice due to their low cost, low heat capacity and physical/chemical properties when they are buried at an optimum depth in the ground. In greenhouse applications, buried pipes are to carry the exhausted humid air from the greenhouse; then, the air flowing through the pipes is either heated or cooled according to the requirement. This depends on the temperature difference between the inside greenhouse air and the inside surface temperature of the buried PVC or HDPE pipes. The mass flow rate, which depends on the cross-sectional area of the pipe and air velocity, can be optimized for a given greenhouse volume. This arrangement is generally referred to as the closed-loop earth–air heat exchanger (CL-EAHE). Such an arrangement has been implemented and evaluated for heating/cooling greenhouses by many researchers [17–23]; however, a survey of the literature revealed that there is a lack of and unclear information about CL-EAHEs operated in gravel–sand soil and arid climates (such as in the KSA). Moreover, because the buried pipes of CL-EAHEs carry humid greenhouse air, water vapour condensation inside the pipes is possible during the cooling process. This possibility needs to be examined for greenhouse applications. Another arrangement, called open-loop earth–air heat exchanger (OL-EAHE), is out of the scope of the present study. This is because, in the OL-EAHE, the preconditioned greenhouse air is usually discharged to the surrounding area outside the greenhouse (i.e., energy and water vapor losses) during the heating and cooling processes of inside greenhouse air. Accordingly, the main objectives of this study are (i) to experimentally measure the temperature profile at different depths inside the ground at the King Saud University campus (as a desert in an arid climate) to determine the optimum depth for burying EAHE pipes; (ii) to examine the possibility of condensation inside the buried pipes; and (iii) to evaluate the maximum heating and cooling potential of the geothermal energy in the KSA for possible use in greenhouses and other domestic and residential building applications.

2. Methodology

2.1. Study Area

The experiment was conducted at the Agricultural Research and Experiment Station, Agriculture Engineering Department, King Saud University (Riyadh, Saudi Arabia; 46″43′ E longitude and 24″38′ N latitude). The soil at the site of the experiment, as well as that of most of arid regions such as the Arabian Peninsula, is composed of gravelly sand and dries up to a 5-m depth or more. Therefore, mechanical digging was used to prepare a hole with a surface area of about 1 m^2 and a depth of 3.5 m. In order to protect the cables of temperature sensors in the soil, these cables were collected to pass through a 5-cm diameter PVC pipe, installed vertically and fixed at the bottom of the hole with a concert block (Figure 1).

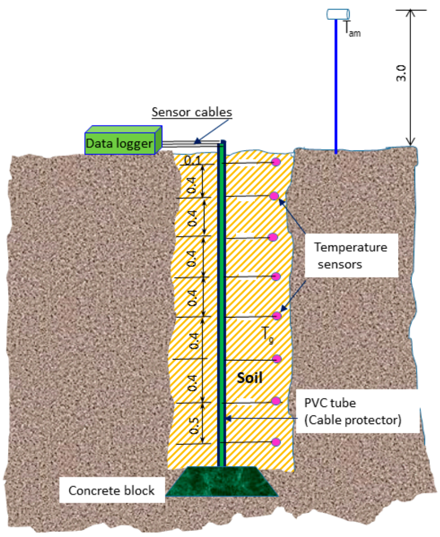

Figure 1. Schematic diagram showing the hole dug into the ground and the locations of thermocouples used to measure underground temperatures (T_g) and ambient temperature (T_{am}).

2.2. Measuring Underground Temperature Profiles

To determine the optimum depth at which the CL-EAHE pipes should be buried, the temperature profile of underground soil was measured at different depths. The optimum location for burying pipes is where the soil temperature became constant, unaffected by the diurnal and seasonal variations in the climatic parameters (GUT). The experiment was conducted during the period from 1 November 2020 to 31 October 2021, to measure the temperatures at the depths of 0.1, 0.5, 0.9, 1.3, 1.7, 2.1, 2.5 and 3 m, in addition to ambient air temperature. Digging up to only a 3.5-m depth was considered because more digging is quite hard and expensive due to the hard nature of soil in the desert of the KSA (i.e., mixture of gravelly sand and rocks). Moreover, the annual variation in soil temperature, T_g ($T_{g,max}$–$T_{g,min}$) at the 3-m depth was expected to be low. Eight small holes were made vertically in the pipe wall (Figure 1) at the levels of measurement (3, 2.5, 2.1, 1.7, 1.3, 0.9, 0.5 and 0.1 m below the ground surface). These holes were to create a path for the allocation of the cables of the temperature sensors and to protect the cables to reach the data logger above the ground via the pipe in a safe (Figure 1). The sensors were inserted into the soil 0.8 m apart from the vertical pipe. The backfilling of the ground hole was performed in steps. The first filling was up to a 3-m depth; then, the temperature sensor was fixed carefully on the soil surface; after that, the second backfilling was made at the level of a 2.5-m depth; then, the temperature sensor was inserted, etc. Thermocouple sensors (wzp-035 Pt100/k; Shenzhen More-Suns Electronics Co., Ltd., Shenzhen, China) were used to measure the underground temperature at the specified locations. The thermocouple had a precision of ±0.1 °C and a temperature range of 0~85 °C. Measurements were taken every 5 min, averaged at every 15 min and recorded in a COMBILOG-1022 data logger (32 channels; Theoder Friedrichs & Co., Schenefeld, Germany).

Due to difficulties and to the high cost of digging, the vertical variation in T_g at different depths and at any time was calculated using the Kasuda formula [24]. Assuming homogeneous soil with a constant thermal diffusivity (α_s), the monthly averaged soil temperature (T_g) at any depth (z) and month number (t) can be estimated by using the following formula:

$$T_g(z,t) = T_m - T_{amp} \times Exp\left[-z\sqrt{\left(\frac{\pi}{12\alpha_s}\right)}\right] \times cos\left\{\frac{2\pi}{12}\left[t - t_o - \frac{z}{2}\sqrt{\frac{12}{\pi\alpha_s}}\right]\right\} \quad (1)$$

where T_g (z,t) is the soil temperature at depth z and month number t; T_m is the annual mean soil surface temperature (°C); T_{amp} is the amplitude of the soil surface temperature [(max − min)/2] in (°C); z is the depth below the ground surface (m); α_s is the ground soil thermal diffusivity (m^2/month); t is time (the month number that the ground temperature is calculated for); t_o is the time shift (month of the year of the lowest ground surface temperature). For the desert of the KSA, the value of α_s was estimated as 2.736 (m^2/month) and thermal conductivity of soil as 2.2–2.8 ($W\ m^{-1}\ °C^{-1}$) [7,8]. From 1 November 2020 to 31 October 2021, the values of T_m and T_{amp} were estimated (from measurements) to be 30 and 12 °C, respectively. Moreover, in January, the lowest ground surface temperatures were recorded; then, t_o, in Equation (1), is equal to one.

2.3. Possibility of Condensation in the Buried CL-EAHE Pipes

In the summer months, the inner surface temperature of the buried EAHE pipes is expected to be much lower than the temperature of the humid air exhausted from the greenhouse. This makes the geothermal effect for cooling inside greenhouse air possible. In summer, when humid air flowing through the buried pipes may cool to its dew-point temperature (T_{dp}) through contact with the inner surface of the pipe, which is cooler than the air, water vapour condenses on the pipe surface. In this case, design considerations should be taken into account to collect the condensed water from the buried EAHE pipes. This may increase the EAHE's cost; therefore, an accurate calculation for T_{dp} is important for the appropriate design of a low-cost CL-EAHE. To examine the possibility of condensation, an experiment was conducted to measure the dry-bulb temperature (T_d) and relative humidity (*RH*) of the ventilated humid air at the greenhouse outlet (exactly before the exhaust fans). A crop-free greenhouse with a floor area of 165 m^2 was used; it was covered with a double-layered polycarbonate sheet of an 8.15-mm thickness. The greenhouse was mechanically ventilated using two exhaust fans, each with an airflow rate of 350 m^3 min^{-1}, operated in summer (July 2021) and in winter (December 2020) to obtain data for two extreme weather conditions, in Riyadh, KSA. T_d and *RH* were measured using a DMA033 Thermo-hygrometer (LSI-Lastem, Milano, Italy). The parameters were measured every 1 min, averaged at every 15 min and recorded in a data logger (CR23X Micro logger, Campbell Scientific, Inc., Oldenburg, Germany). The well-known approximate formulation used to calculate the dew-point temperature (T_{dp}) is based on Magnus' formula [25], for which the measured T_d (in °C) and *RH* (%) are required; then, the saturated water vapour pressure (P_s in Pascal) corresponding to T_d is given, by [25], as follows:

$$P_s = 610.78 \times Exp\left(\frac{17.2694 \times T_d}{(T_d + 238.3)}\right) \quad (2)$$

The actual water vapour pressure (P_a, in Pascal) is given by the following:

$$P_a = P_s \times RH(\%)/100 \quad (3)$$

$$S = ln(P_a/610.78) \quad (4)$$

$$T_{dp} = S \times 238.3/(17.294 - S) \quad (5a)$$

Another simple approximation is used to calculate T_{dp} (°C) for *RH* > 50% and ±1 °C error [26], in the following form:

$$T_{dp} = T_d - \left(\frac{100 - RH}{5}\right) \quad (5b)$$

These approximations are commonly used to calculate T_{dp}; however, in arid climates (where T_d is very high and *RH* is very low), the validity of these approximations ((Equation (5a,b)) needs to be examined specifically for the arid climate.

For greater accuracy, the saturation water vapour pressure (P_s) has been modified and Equation (5a) enhanced, becoming known as an Arden Buck equation [27], by which the modified saturation water vapour pressure (P_{sm}, in Pascal) corresponding to a dry bulb temperature of air (T_d, in °C) is given by the following:

$$P_{sm} = a \times Exp\left\{\left(b - \frac{T_d}{D}\right)\left(\frac{T_d}{c + D}\right)\right\} \quad (6)$$

$$T_{dp} = \frac{c \times ln\left(\frac{RH}{100} \times \frac{P_{sm}}{a}\right)}{b - ln\left(\frac{RH}{100} \times \frac{P_{sm}}{a}\right)} \quad (7)$$

The constants in Equations (6) and (7) were provided with a maximum error of ≤0.05% and T_d from 0 up to 50 °C as follows: *a* = 611.21 Pa, *b* = 17.368, *c* = 238.88 °C and *D* = 234.5 °C [27].

2.4. Geothermal Cooling/Heating Capacity

In an EAHE, the PVC or HDPE pipes are buried permanently under the ground at a specified location, where the ground temperature (T_g) is annually stable and nearly constant; therefore, the thermal conditions can be characterized as steady state and equilibrium. Moreover, the thickness of an EAHE pipe is very modest (e.g., 4.25 mm) compared to the pipe surface area or the pipe diameter (203.2 mm). Hence, for simplicity, we assumed that the thermal resistance of the pipe material was negligible, and the inner surface temperature of the pipe (T_s) was almost uniform and constant along the axial direction of pipe and equal, in most cases, to the ground temperature (T_g) at the pipe location. The cooling and heating capacity of an EAHE ($\dot{Q}_{c/h}$) is defined as follows:

$$\dot{Q}_{c/h} = \dot{m}_a C_p \left(T_{out} - T_{in}\right) \tag{8}$$

where $\dot{m}_a$ is the mass flow rate of air exhausted from the greenhouse (ventilation rate at T_{ex}) and flowing through the EAHE pipes (kg s^{-1}); C_p is the specific heat capacity of air (J kg^{-1} $°C^{-1}$); and T_{in} and T_{out} are the temperatures of the inlet and outlet air (°C) for the EAHE pipes. T_{in} is assumed to be the temperature of air exhausted from the greenhouse (T_{in} = T_{ex} in °C) and it can be obtained directly from measurements. For a very long pipe, T_{out} is assumed to be equal to the inner surface temperature of the EAHE pipes (i.e., T_{out} = T_s = T_g). In this case, Equation (8) represents the maximum cooling/heating capacity that can be provided by an EAHE ($Q_{c/h,max}$). In a similar manner, the cooling/heating potential ($Q_{c/h}$), in Joules, over a specified period is defined, by [17,18], as follows:

$$Q_{c/h} = \sum_{time} \dot{m}_a C_p (T_{out} - T_{in}) \Delta t \tag{9}$$

where Δt is the time interval (s). In fact, the outlet air temperature of EAHE pipes (T_{out}) is lower than the ground temperature (T_g) or the inner surface temperature of the pipes (T_s); this depends on the effectiveness of the EAHE. Therefore, an expression for T_{out} in terms of underground temperature (T_g) and inlet temperature of air (T_{in}) is given, by [13], as follows:

$$T_{out} = T_g \left\{ 1 - exp\left(-\frac{A_s h_f}{\dot{m}_a C_p} \right) \right\} + T_{in} exp\left(-\frac{A_s h_f}{\dot{m}_a C_p} \right) \tag{10}$$

where A_s is the inner surface area of a single pipe in the EAHE; $\dot{m}_a$ and C_p are the mass flow rate and specific heat of air flowing in a single pipe (kg s^{-1} and J kg^{-1} $°C^{-1}$); and h_f is the convective heat transfer coefficient between the inner surface of the pipe and the flowing air (W m^{-2} $°C^{-1}$). h_f is a critical parameter in the EAHE design; in such a case, it is reasonable to assume that the air flow in the EAHE pipes is fully developed. To adapt an appropriate correlation to calculate h_f, Bisoniya [13] examined eight Nusselt number (Nu) correlations and recommended the following correlation for turbulent flows in a pipe with a smooth internal surface [13]:

$$N_u = \frac{f/8(R_e - 1000)P_r}{1 + 12.7\sqrt{(f/8)}\left(P_r^{2/3} - 1\right)} \tag{11}$$

The friction coefficient f for turbulent flow is given by the following:

$$f = (1.82\, logR_e - 1.64)^{-2}, \left(2300 \le R_e < 5 \times 10^6\right) \text{ and } \left(0.5 < P_r < 10^6\right) \tag{12}$$

where the Reynolds number ($R_e = dv\rho/\mu$) and Prandtl number ($P_r = \mu C_p/k$) are calculated for the air flowing through a pipe; d is the inner diameter of the pipe; v is the air velocity in the pipe; ρ is the air density; μ is the air viscosity; and k is the thermal conductivity of air. The unit of each parameter was adjusted to give dimensionless numbers (Nu, Re and Pr).

By determining the value of h_f, Equation (10) can be used as a design tool to optimize the number of pipes and the length and diameter of each pipe for the EAHE design.

3. Results and Discussion

3.1. Underground Soil Temperature

It is well known that the ground temperature is affected by the cyclic variation in climatic parameters such as solar radiation, ambient air temperature, wind speed, humidity, rainfall and snow, if any, etc. The interaction between the climatic parameters and the ground is mainly at the ground surface; then, the cyclic variation in the ground temperature (T_g) decreases as the ground depth increases. At a certain depth, according to the chemical/physical properties of soil, T_g becomes nearly constant, unaffected by the diurnal and seasonal variations in the climatic parameters, and it is defined as the ground undisturbed temperature (GUT). The GUT is an essential parameter in designing an EAHE system. It is quite difficult to theoretically calculate the GUT correctly, because it depends on the soil parameters and the climatic conditions affecting the ground surface. Therefore, an experiment was conducted (Section 2) for measuring T_g at different ground depths during different seasons to determine the depth at which T_g became nearly constant throughout the year (GUT). To illustrate the daily cyclic variation in ambient air and soil temperatures during the period of the experiment (from 1 November 2020 to 31 October 2021), four days were selected to represent the extreme weather conditions, two days in cold winter (29–30 December) and two days in hot summer (30–31 July). The measured parameters (i.e., T_{am} and T_g at different depths) are depicted in Figure 2 (for winter days) and in Figure 3 (for summer days). In winter, the ground temperature (T_g) increased as the ground depth increased (Figure 2) and the opposite observation was noted in summer (Figure 3). In Figures 2 and 3, the cyclic variation in T_g is significant at a 0.1-m depth as affected by the diurnal variation in the climatic parameters (mainly the solar irradiance and T_{am}) in summer and winter. At a depth from ≥0.5 m up to 3 m, T_g became nearly constant in summer and in winter and was not affected by the diurnal variation in the climatic parameters. At a 3-m depth, T_g was about 29 °C in winter (Figure 2) and about 32 °C in summer (Figure 3) and a difference of 3 °C in the T_g value is acceptable between the hot summer and cold winter seasons. For more clarification and to find the optimum depth for burying the EAHE pipes, the vertical variation in the monthly average soil temperature (T_g) at different depths for the experimental site (Riyadh, KSA) is plotted in Figure 4 and the annual variation in temperatures of ambient air (T_{am}) and soil (T_g) at the 0.5-m and 3-m depths is plotted in Figure 5. As illustrated in Figures 4 and 5, at the 3-m depth, the maximum annual variation (max − min) in T_g was about 5 °C. The lowest value of T_g was around 27 °C in February and March and the highest value of T_g was around 32 °C in September and October. This annual variation in T_g (29–32 °C) is adequate for heating and cooling purposes and can be considered as the GUT and the depth of 3 m is adequate for burying the EAHE pipes. The annual variation in T_g is considerable at the 0.5-m depth; more stability of T_g was observed at the 3-m ground depth (Figure 5). According to Figure 5, the heating effect of a supposed EAHE in winter is expected to be relatively higher than its cooling effect in summer; this depends on the temperature difference between T_{am} and GUT (T_g at the 3-m depth).

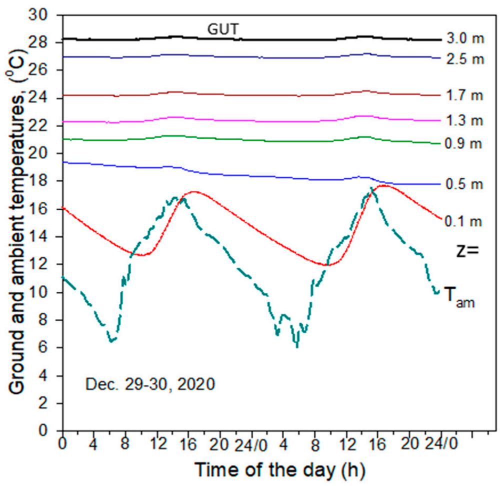

Figure 2. Diurnal variation in ambient temperature (T_{am}) and underground soil temperature (T_g) at different depths (z) in winter season (29–30 December 2020).

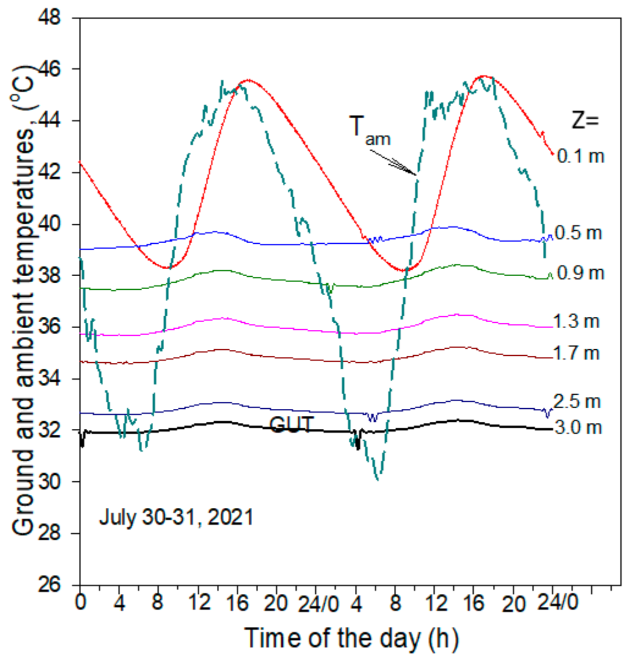

Figure 3. Diurnal variation in ambient temperature (T_{am}) and underground soil temperature (T_g) at different depths (*z*) in summer season (30–31 July 2021).

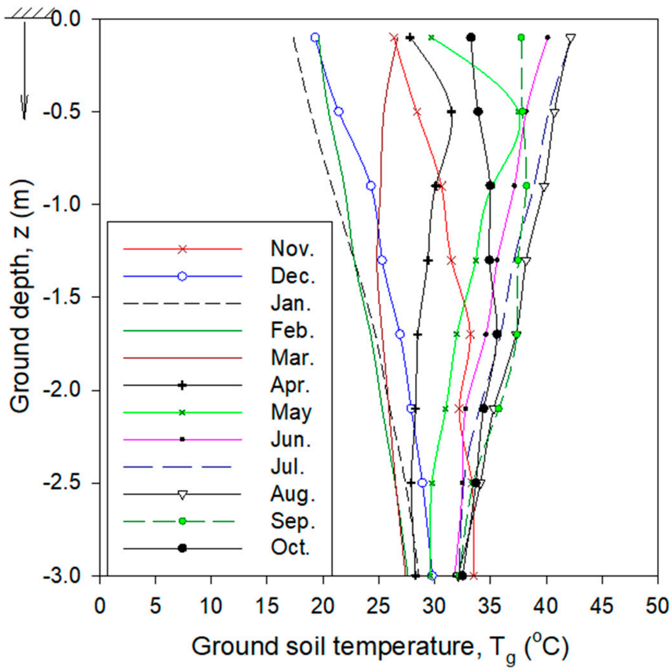

Figure 4. Vertical variation in the monthly average ground temperature (T_g) at different depths (*z*) for Riyadh region, KSA, in the years 2020–2021.

As farther digging in the desert of arid regions is quite difficult and expensive, we used Equation (1) to predict the monthly average values of T_g at different depths. To calculate the values of T_m and T_{amp} in Equation (1), the measured T_g at the 0.1-m depth was considered as the soil surface temperature. The predicted results for 12 months and depths of >3 m are plotted in Figure 6. As illustrated in Figure 6, at a depth (*z*) greater than 13 m, T_g becomes constant at 30 °C throughout the year. As the arid climatic condition is almost similar every year in the deserts of KSA, the GUT can be considered constant at 30 °C throughout the year at a depth greater than 13 m.

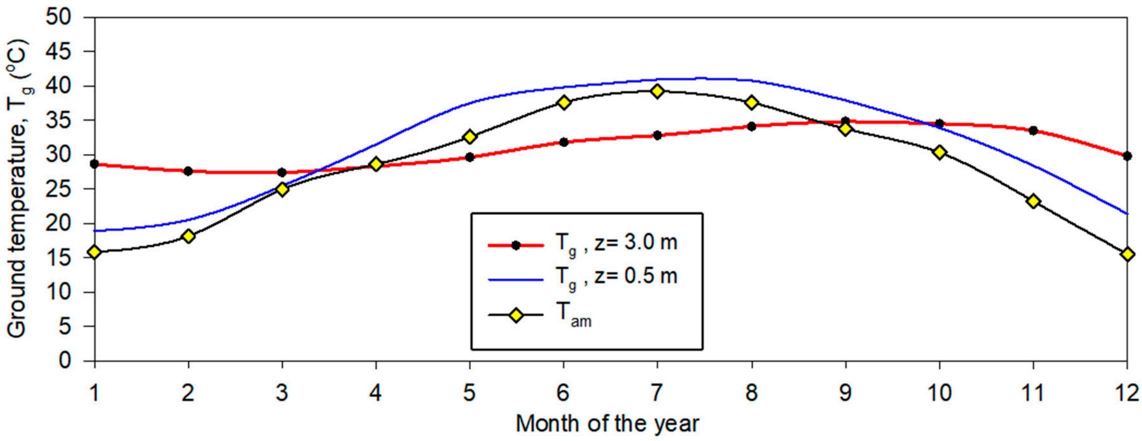

Figure 5. Annual variation in temperatures of ambient air (T_{am}) and ground soil (T_g) at 0.5- and 3.0-m depths for Riyadh, Saudi Arabia.

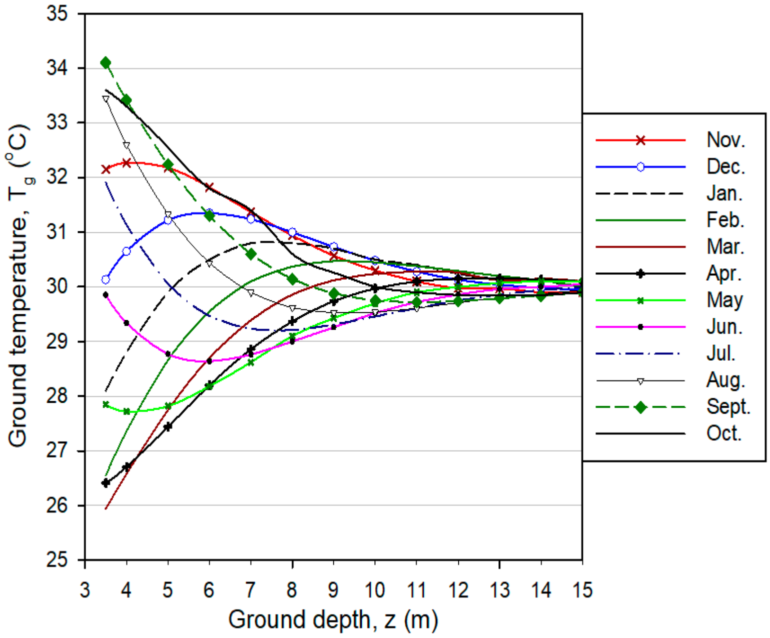

Figure 6. Ground temperature variation (monthly average) with depth, predicted using Equation (1) for the KSA desert.

3.2. Possibility of Condensation in the EAHE Pipes

The proposed CL-EAHE was applied in a greenhouse for cooling/heating purposes in the summer and winter seasons. In the cooling/heating processes, humid air is exhausted from the greenhouse (at T_{ex} and RH_{ex}); it flows in the buried pipes, then the condensation of water vapour in the pipes is possible during cooling. The occurrence of condensation requires extra design consideration to collect the condensed water from the pipes. The most accurate correlation (Equation (7)) was used to calculate the dew-point temperature (T_{dp}) of the exhausted air (having T_{ex} and RH_{ex}) for the four previously selected days (hot and dry in summer and humid and cold in winter). No heating or cooling was applied to the greenhouse to represent the actual practical situations. Figures 7 and 8 illustrate the diurnal variation in the measured T_{ex} and RH_{ex} for the exhausted air from the greenhouse, the measured GUT (T_g at the 3-m depth) and the calculated T_{dp} (using Equation (7)). A considerable difference could be observed between T_{ex} and T_{dp} in summer (Figure 8) and in winter (Figure 7). For winter heating (Figure 7), T_{ex} increased, as affected by the warm inner surface of the EAHE pipes; if the upper limit of T_{ex} was to reach the GUT, then the gap between the T_{ex} and T_{dp} of the air would increase and the condensation of water vapour would be impossible. For summer cooling (Figure 8), if T_{ex} was to decrease to its lower limit GUT (i.e., T_g at the 3-m depth), there would still be a large difference between T_{ex} and T_{dp} (Figure 8); therefore, condensation would never take place or would be impossible. Moreover, a large number of combinations for T_{ex} and RH_{ex} was used to calculate T_{dp} using Equation (7) and the resulting values of T_{dp} do not exceed 20 °C; in each combination, a large difference between T_{ex} and T_{dp} remained. Accordingly, condensation in CL-EAHE pipes would be impossible throughout the year for the pipes buried at a 3-m depth in the Riyadh area, KSA.

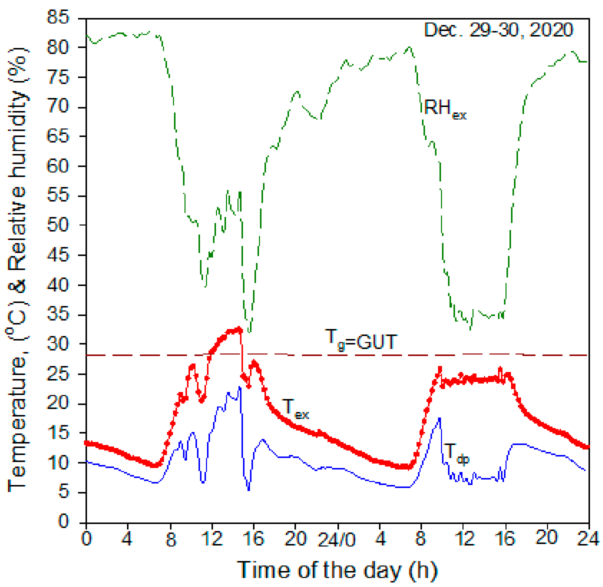

Figure 7. Diurnal variation in estimated dew-point temperature (T_{dp}) of air ventilated from a greenhouse at T_{ex} and RH_{ex} and flowed through EAHE pipes buried at the GUT in winter season (29–30 December 2020).

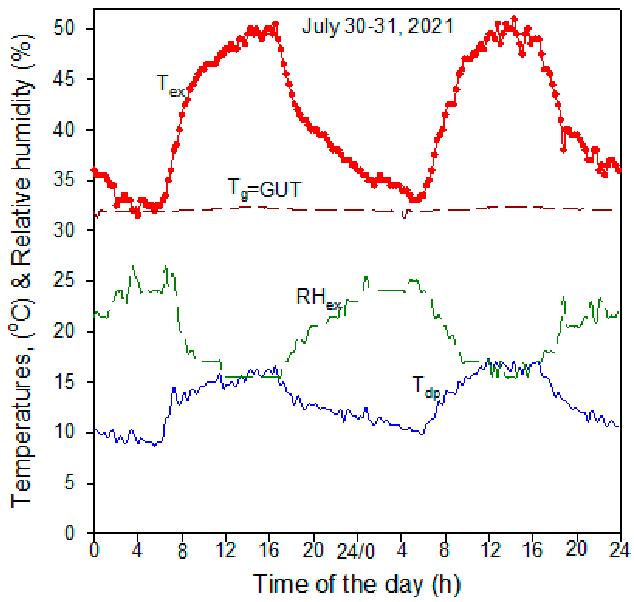

Figure 8. Diurnal variation in estimated dew-point temperature (T_{dp}) of air ventilated from a greenhouse at T_{ex} and RH_{ex} and flowed through EAHE pipes buried at the GUT in summer season (30–31 July 2021).

Similarly, T_{dp} was calculated using Equation (5a,b) to check the validity of these approximations to be used to calculate T_{dp} for an arid climate. The percentage error, E_R (%), was calculated in each case as E_R (%) = abs{($T_{accurate}$-$T_{approximate}$)/$T_{accurate}$} × 100. The values of E_R (%) were calculated for a wide range of T_d and RH and are plotted in Figure 9a,b for Equation (5a) and in Figure 10 for Equation (5b). Based on Figure 9a,b, Equation (5a) can be used to calculate T_{dp} with an error less than 1% for RH > 40% and T_d < 30 °C. However, Equation (5b) can be used only for RH > 60% with an error of about 3–4%; for low RH values (as in the arid climate), such an approximation (Equation (5b)) cannot be used. Accordingly, for arid climatic conditions (as in the Arabian Peninsula region), such approximations (Equation (5a,b)) are not recommended and Equation (7) is the appropriate correlation to determine T_{dp} correctly.

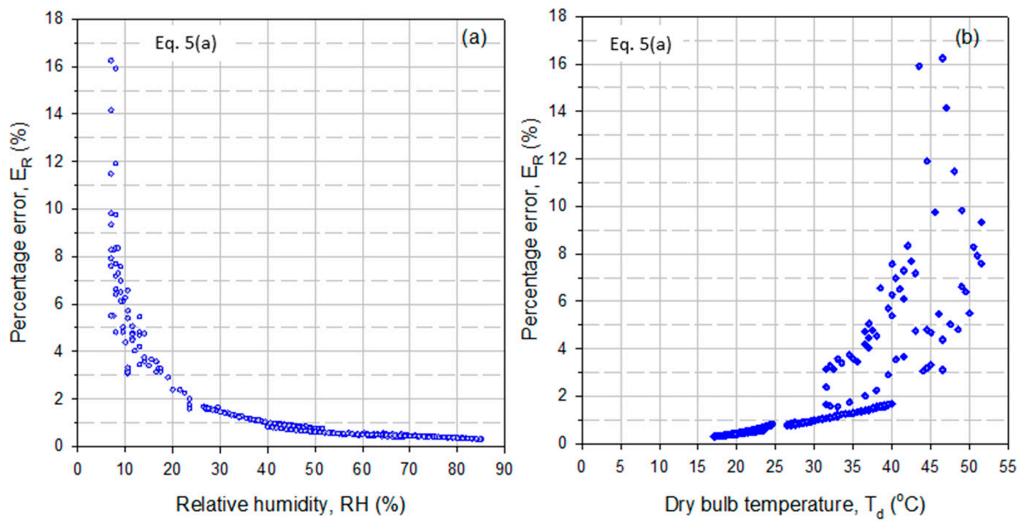

Figure 9. Percentage error, E_R (%), in the approximated value of T_{dp} (estimated by using Equation (5a)) as affected by (**a**) relative humidity (RH) and (**b**) dry bulb temperature (T_d).

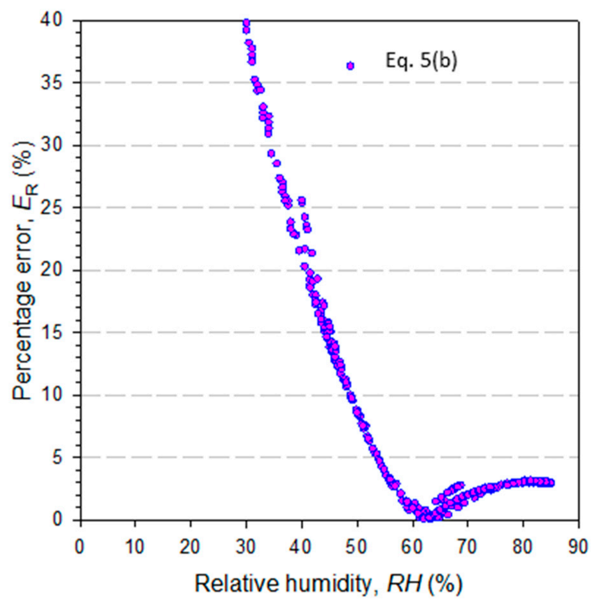

Figure 10. Percentage error, E_R (%), in the approximated value of T_{dp} (estimated by using Equation (5b)) as affected by relative humidity (RH).

3.3. Maximum Cooling/Heating Capacity

An EAHE's geothermal energy potential, as well as its cooling/heating capacity, depends mainly on the climatic parameters and the underground soil conditions. For EAHE pipes buried at a specified optimum depth, T_g equals the GUT. Under the steady-state thermal condition, the inner surface temperature of the pipe (T_s) is assumed to be uniform in the axial flow direction and by assuming the thermal resistance of the pipe material is negligible, the equality $T_s = T_g$ = GUT can be assumed with insignificant error. If the pipe is long enough, the outlet air temperature (T_{out}) from the pipe can be assumed to be equal to T_s ($T_{out} = T_s = T_g$ = GUT). In this case, the EAHE provides its maximum possible cooling/heating capacity. Therefore, in Equation (8), T_{in} and T_{out} were taken as T_{ex} (exit air from the greenhouse) and GUT, respectively; $\dot{Q}_{c/h,max}$ was estimated per cubic meter of airflow. For winter cooling, a considerable amount of heat is expected to be added to the flowing air at around midnight (Figure 11). In addition, at around noon, in winter, operating the EAHE is not necessary and the transmitted solar radiation into the greenhouse is enough for warming up the inside air. In summer, a considerable amount of heat is expected to be removed from the flowing air at around noon; however, at around midnight, it is not necessary to operate the EAHE (Figure 11). Under the presumed ideal conditions and to estimate the maximum possible cooling/heating potential that the ground (at a 3-m depth) can provide in the cold winter and hot summer in the Riyadh region, the results are integrated in Figure 11. The expected maximum possible cooling and heating potential are 890 and 1000 MJ m^{-3} day^{-1}, respectively. These values are promising to use EAHEs for different applications in the KSA and the Arabian Peninsula regions.

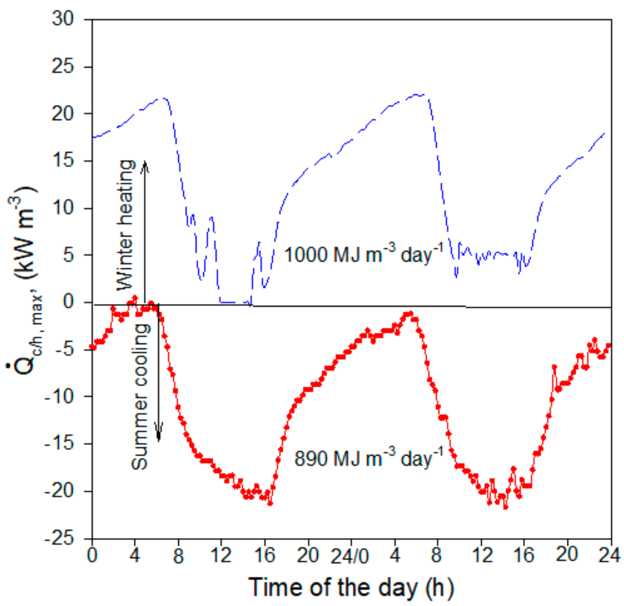

Figure 11. Diurnal variation in maximum cooling/heating capacity ($\dot{Q}_{c/h,max}$) that an EAHE can provide and the maximum cooling/heating potential per day.

4. Conclusions

This study is an attempt to provide critical information for EAHE designers and to evaluate the geothermal energy potential for possible cooling/heating greenhouses and indoor spaces in hot arid regions, for which two experiments were conducted. The main conclusion is summarized below.

The daily cyclic variation in the climatic parameters affected the ground temperature (T_g) up to a 0.5-m depth, after which T_g was constant daily; it increased with depth in winter and decreased with depth in summer.

At a 3-m depth, the annual variation in T_g was minor and it can be considered as the ground undisturbed temperature, GUT. The GUT value was 29 °C in winter and 32 °C in summer; these values are adequate for cooling/heating purposes in a climate in which the ambient air temperature drops below 10 °C on winter nights and exceeds 47 °C on summer days. For an EAHE operating under ideal conditions, the geothermal energy level can provide a maximum cooling/heating potential of 890/1000 MJ per m^3 of flowing air per day.

In summer seasons, during the cooling process of greenhouse air in EAHE pipes distributed at a 3-m depth, the condensation of water vapor in the pipes could never take place.

In arid climates, approximate correlations (Equation (5a,b)) are not recommended to calculate the dew-point temperature of air (T_{dp}). However, Equation (7) is the appropriate correlation to determine T_{dp} correctly.

The geothermal energy potential is promising for cooling/heating applications in arid regions such as the Arabian Peninsula for sustainable development and environmental protection. Further research should be conducted to design, construct and operate an EAHE connected to a greenhouse and evaluate the system performance under different operating and climate conditions.

Author Contributions: Conceptualization and methodology, A.A.-G. and I.A.-H.; validation, A.A., S.M. and A.I.; formal analysis, A.A.-G., S.M. and I.A.-H.; investigation, A.A.-G.; resources, M.S.; data creation, M.S., S.M. and A.I.; writing—original draft preparation, I.A.-H., S.M. and A.I.; writing—review and editing, A.A.-G.; visualization, M.S., S.M. and A.I.; supervision, A.A.-G.; project administration, I.A.-H. All authors have read and agreed to the published version of the manuscript.

Funding: This research study received no external funding.

Acknowledgments: The authors extend their appreciation to the Deputyship for Research and Innovation, Ministry of Education in Saudi Arabia, for funding this research work through the project number DRI-KSU-542.

Conflicts of Interest: The authors declare no conflict of interest.

Nomenclature

Symbol	*Description*	*(unit)*
A_s	Inner surface area of EAHE pipe	(m^2)
C_p	Specific heat of flowing air through EAHE pipes	(J kg^{-1} $°C^{-1}$)
d	Inner diameter of the EAHE pipes	(m)
E_R	Percentage error	(%)
h_f	Convective heat transfer coefficient between inner surface of EAHE pipe and flowing air	(W m^{-2} $°C^{-1}$)
k	Thermal conductivity of flowing air	(W m^{-1} $°C^{-1}$)
L	Length of one EAHE pipe	(m)
$\dot{m}_a$	Mass flow rate of flowing air through EAHE pipes	(kg s^{-1})
N_u	Nusselt number	$(N_u = dh/k)$
P_a	Actual water vapor pressure	(Pa)
P_r	Prandtl number	$(P_r = \mu C_{pa}/k)$
P_s	Saturation water vapor pressure	(Pa)
$\dot{Q}_{c/h}$	Cooling/heating capacity	(W)
$Q_{c/h}$	Cooling/heating potential	(J)
R_e	Reynolds number	$(R_e = dv\rho/\mu)$
RH	Relative humidity of air	(%)
RH_{ex}	Relative humidity of air exhausted from the greenhouse	(%)
t	Time	(s; day; month)
T_{amp}	Amplitude of the annual ground surface temperature	(°C)
T_d	Dry bulb temperature of air or ambient temperature (T_{am} = T_d)	(°C)
T_{dp}	dew point temperature of flowing air in the EAHE pipe	(°C)
T_{ex}	Temperature of air exhausted from the greenhouse	(°C)

T_g	Underground soil temperature	(°C)
T_{in}	Inlet hot/cold air temperature to the EAHE pipes	(°C)
T_m	Mean ground surface temperature, annual average	(°C)
T_{out}	Outlet hot/cooled air temperature from the EAHE pipes	(°C)
T_s	Outlet hot/cooled air temperature from the EAHE pipes	(°C)
v	Velocity of flowing air through EAHE Pipe	(m s^{-1})
z	Depth below the soil surface	(m)
Greek letter		
α_s	Thermal diffusivity of soil	(m^2/day)
ρ	Density of flowing air through EAHE pipe	(kg m^{-3})
μ	Dynamic viscosity of flowing air through EAHE pipe	(kg m^{-1} s^{-1})
Δt	Interval of time	(s, h, day, etc.)
Abbreviations		
CL-EAHE	Closed-loop earth to air heat exchanger	
EAHE	Earth to air heat exchanger	
KSA	the Kingdom of Saudi Arabia	
OL-EAHE	Open loop earth to air heat exchanger	
GUT	Ground undisturbed temperature	(°C)

References

1. Abdel-Ghany, A.M.; Picuno, P.; Al-Helal, I.M.; Alsadon, A.; Ibrahim, A.; Shady, M. Radiometric characterization, solar and thermal radiation in a greenhouse as affected by shading configuration in an arid climate. *Energies* **2015**, *8*, 13928–13937. [CrossRef]
2. Al-Helal, I.M.; Al-Hamdan, A.M. Effect of arid environment on radiative properties of greenhouse polyethylene cover. *Sol. Energy* **2009**, *83*, 790–798. [CrossRef]
3. Alkoaik, F.N.; Al-Faraj, A.A.; Al-Helal, I.M.; Ronnel, B.F.; Mansour, N.I.; Abdel-Ghany, A.M. Toward sustainability in rural areas: Composting palm tree residues in rotation bioreactors. *Sustainability* **2019**, *12*, 201. [CrossRef]
4. El Haj, A.M.; Sadeghzadeh, M.; Ahmadi, M.H.; Al-Shabi, M.; Albawab, M.; Anvari-Moghaddam, A.; Bani-Hani, E. Space cooling using geothermal single-effect water/lithium bromide absorption chiller. *Energy Sci. Eng.* **2021**, *9*, 1747–1760. [CrossRef]
5. El Haj, A.M.; Aryanfar, Y.; Radman, S.; Yousef, B.; Pakatchian, M. Energy and exergy analyses of single flash geothermal power plant at optimum separator temperature. *Int. J. Low-Carbon Technol.* **2021**, *16*, 873–881.
6. El Haj, A.M.; Aryanfar, Y.; Javaherian, A.; Khosravi, A.; Aghaei, K.; Hosseinzadeh, S.; Pabon, J.; Mahmoudi, S.M.S. Energy, exergy, economic and exergoenvironmental analyses of transcritical CO_2 cycle powered by single flash geothermal power plant. *Int. J. Low-Carbon Technol.* **2021**, *16*, 1504–1518. [CrossRef]
7. Demirbas, A.; Alidrisi, H.; Ahmed, W.; Sheikh, M.H. Potential of geothermal energy in the Kingdom of Saudi Arabia. *Energy Sources Part A Recovery Util. Environ. Eff.* **2016**, *38*, 2238–2243. [CrossRef]
8. Lashin, A.; Al Arifi, N. Geothermal energy potential of southwestern of Saudi Arabia "exploitation and possible power generation": A case study at AlKhouba area-Jazan. *Renew. Sustain. Energy Rev.* **2014**, *30*, 771–789. [CrossRef]
9. Bharadwaj, S.S.; Bansal, N.K. Temperature distribution inside ground for various surface conditions. *Build. Environ.* **1981**, *16*, 183–192. [CrossRef]
10. Vidhi, R. A review of underground soil and night sky as passive heat sink: Design configurations and models. *Energies* **2018**, *11*, 2941. [CrossRef]
11. Díaz-Hernández, H.P.; Macias-Melo, E.V.; Aguilar-Castro, K.M.; Hernández-Pérez, I.; Xamán, J.; Serrano-Arellano, J.; López-Manrique, L.M. Experimental study of an earth to air heat exchanger (EAHE) for warm humid climatic conditions. *Geothermics* **2020**, *84*, 101741. [CrossRef]
12. Hermes, V.F.; Ramalho, J.V.A.; Rocha, L.A.O.; Santos, E.D.; Marques, W.C.; Costi, J.; Rodrigues, M.K.; Isoldi, L.A. Further realistic annual simulations of earth-air heat exchangers installations in a coastal city. *Sustain. Energy Technol. Assess.* **2020**, *37*, 100603. [CrossRef]
13. Bisoniya, T.S. Design of earth–air heat exchanger system. *Geotherm Energy* **2015**, *3*, 18. [CrossRef]
14. Cao, S.; Li, F.; Li, X.; Yang, B. Feasibility analysys of earth-air heat exchanger (EAHE) in a sports and culture centre in Tianjin, China. *Case Stud. Therm. Eng.* **2021**, *26*, 101654. [CrossRef]
15. Le, A.T.; Wang, L.; Wang, Y.; Li, D. Measurement investigation on the feasibility of shallow geothermal energy for heating and cooling applied in agricultural greenhouses of Shouguang City: Ground temperature profiles and geothermal potential. *Inf. Process. Agric.* **2021**, *8*, 251–269. [CrossRef]
16. Hebbal, B.; Marif, Y.; Hamdani, M.; Belhadj, M.M.; Bouguettaia, H.; Bechki, D. The geothermal potential of underground buildings in hot climates: Case of southern Algeria. *Case Stud. Therm. Eng.* **2021**, *28*, 101422. [CrossRef]
17. Tiwari, G.N.; Akhtar, M.A.; Shukla, A.; Emran Khan, M. Annual thermal performance of greenhouse with an earth-air heat exchanger: An experimental validation. *Rene Energy* **2006**, *31*, 2432–2446. [CrossRef]

18. Ghosal, M.K.; Tiwari, G.N.; Das, D.K.; Pandey, K.P. Modeling and comparative thermal performance of ground air collector and earth air heat exchanger for heating of greenhouse. *Energy Build.* **2005**, *37*, 613–621. [CrossRef]
19. Stanciu, D.; Stanciu, C.; Paraschiv, I. Mathematical links between optimum solar collector tilts in isotropic sky for intercepting maximum solar irradiance. *J. Atmos. Sol.-Terr. Phys.* **2016**, *137*, 58–65. [CrossRef]
20. Ozgener, O.; Ozgener, L.; Goswami, D.Y. Experimental prediction of total thermal resistance of a closed loop EAHE for greenhouse cooling system. *Int. Commun. Heat Mass Transf.* **2011**, *38*, 711–717. [CrossRef]
21. Ozgener, O.; Ozgener, L.; Goswami, D.Y. Seven years energetic and exergetic monitoring for vertical and horizontal EAHE assisted agricultural building heating. *Renew. Sustain. Energy Rev.* **2017**, *80*, 175–184. [CrossRef]
22. Hepbasli, A. Low exergy modelling and performance analysis of greenhouses coupled to closed earth-to-air heat exchangers (EAHEs). *Energy Build.* **2013**, *64*, 224–230. [CrossRef]
23. Bisoniya, T.S.; Kumar, A.; Baredar, P. Experimental and analytical studies of earth-air heat exchanger (EAHE) systems in India: A review. *Renew. Sustain. Energy Rev.* **2013**, *19*, 238–246. [CrossRef]
24. Kasuda, T.; Archenbach, P.R. Earth temperature and thermal diffusivity at selected stations in the United States. *ASHRAE Trans.* **1965**, *71*, 61–74.
25. NASA Technical Note, NASA TN D-8401, Equations for the Determination of Humidity from Dew Point Ad Psychometric Data. Available online: https://www.nasa.gov/centers/dryden/pdf/87878main_H937.pdf (accessed on 14 August 2021).
26. Dew Point Temperature—An Overview, Science Direct Topics. Available online: https://www.sciencedirect.com/topics/engineering/dewpoint-temperature (accessed on 17 July 2021).
27. Buck, A.L. New equations for computing vapour pressure and enhancement factor. *J. Appl. Meteorol.* **1981**, *20*, 1527–1532. [CrossRef]